Eurographics Workshop on Visual Computing for Biology and Medicine (2012)
T. Ropinski, A. Ynnerman, C. Botha, and J. B. T. M. Roerdink (Editors)

Synaptic Connectivity in Anatomically Realistic Neural Networks: Modeling and Visual Analysis

Vincent J. Dercksen[1], Robert Egger[2,3], Hans-Christian Hege[1] and Marcel Oberlaender[2,3]

[1]Department Visualization and Data Analysis, Zuse Institute Berlin, Berlin, Germany
[2]Digital Neuroanatomy Group, Max Planck Florida Institute, Jupiter, USA
[3]Current affiliation: Computational Neuroanatomy Group, Max Planck Institute for Biological Cybernetics, Tübingen, Germany

Abstract

The structural organization of neural circuitry is an important determinant of brain function. Thus, knowing the brain's wiring (the connectome) is key to understanding how it works. For example, understanding how sensory information is translated into behavior requires a comprehensive view of the microcircuits performing this translation at the level of individual neurons and synapses. Obtaining a wiring diagram, however, is nontrivial due to size, complexity and accessibility of the involved brain regions. Even when such data were available, it were difficult to analyze. Here we describe how a network of ∼0.5 million neurons and their synaptic connections, representing the vibrissal area of the rat primary somatosensory cortex, can be reconstructed. Furthermore, we present a framework for visual exploration of synaptic connectivity between (groups of) neurons within this model. It includes, first, the Cortical Column Connectivity Viewer (CCCV) that provides a hybrid abstract/spatial representation of the connections between neurons of different cell types and/or in different cortical columns. Second, it comprises a 3D view of cell type-specific synapse positions on selected morphologies. This framework is thus an effective tool to visually explore structural organization principles at the population, individual neuron and synapse levels.

1. Introduction

One fundamental question in neuroscience is how brains translate sensory information into behavior. In order to understand such processes it is essential to obtain structural descriptions of the involved microcircuits, its neuronal elements and their synaptic interconnections, the 'connectome' [STK05]. A convenient model system to investigate the relationship between sensory stimuli and behavioral responses is the rodent whisker system (Fig. 1a). Tactile information obtained from a single facial whisker is conveyed via the brainstem and thalamus to the vibrissal area of the primary somatosensory cortex (barrel cortex, S1, Fig. 1b) in a segregated manner, i.e. there is a 1-to-1 correspondence between each whisker and a cortical barrel column [Hel07]. Further, single whisker input is sufficient to trigger simple behaviors, such as decision-making [CS07].

One way to create an anatomically realistic model of the barrel cortex would be by dense reconstruction of neuron morphologies and their synaptic contact sites within one animal from electron-microscopic data. However, dense reconstructions of volumes as large as a cortical column or even the barrel cortex are, at present, not feasible [Hel07, Obe11a]. We therefore use a 'reverse engineering' approach: anatomical information, including spatial neuron distributions and 3D morphologies, obtained from different (light-microscopic) image modalities and different animals is registered into a common reference frame. After placement of axon and dendrite morphologies, the spatial distribution of synaptic contacts between the different cell types and in different columns is estimated based on structural overlap.

Recently, this approach has been applied to create a realistic model of the population of excitatory neurons in a single cortical column [Obe11a, Lan11] and its synaptic innervation by thalamo-cortical (VPM) axons. This model thus allowed for the quantitative and visual analysis of cell type-specific innervation patterns. Here, we extend this model to the entire barrel cortex, including 10 different cell types and

© The Eurographics Association 2012.

DOI: 10.2312/VCBM/VCBM12/017-024

delivered by EUROGRAPHICS DIGITAL LIBRARY www.eg.org diglib.eg.org

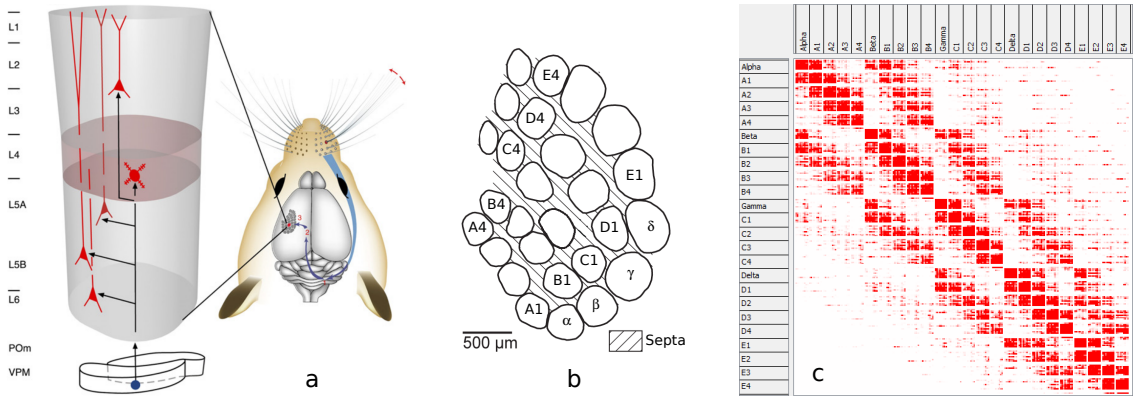

Figure 1: *(a) Sensory input from a whisker is conveyed via brain stem (1) and thalamus (2) to its associated cortical column in S1 (3) (image modified from [Hel07]). (b) Barrel cortex layout as seen from the top. (c) Connectivity matrix visualization by the heatmap view of the framework.*

24 barrel columns, resulting in a network consisting of ∼0.5 million neurons and their synaptic connections (see Fig. 1).

Due to the increase in size and complexity, analyzing the synaptic connectivity within such a data set is non-trivial. We present an analysis framework for the interactive investigation of synaptic connectivity. A major component of this framework is the Cortical Column Connectivity Viewer (CCCV), a tool for interactive visualization of the connection strength between (groups of) neurons in cortical columns, using a hybrid spatial/abstract view. Together with a 3D visualization of the sub-cellular distribution of synapses, this framework yields insight into connectivity from the neuron population down to the sub-cellular scale.

2. Neuroscientific Research Questions

The model of the barrel cortex contains a wealth of connectivity information. Important questions that could be answered on the basis of this information include:

- Q1 Where does a neuron or group of neurons obtain input from, i.e. to which presynaptic cells is it connected? Or, conversely, where does a presynaptic group project to?
- Q2 How does thalamic innervation differ between columns and between cell types in the columns?
- Q3 How are synapses distributed on the postsynaptic cell? Can cell type-specific clustering of synapses at particular locations be identified?
- Q4 How large is the input of surrounding columns compared to intra-column input for different cell types?

Answers to these questions would help to identify local (intra-column) and long-range (inter-column) microcircuits involved in processing of tactile information obtained from single or multiple whiskers. Furthermore, at the subcellular level, cell type-specific distributions of synapses may be directly compared to functional imaging data [Var11] to understand how cell function relates to its structural properties.

3. Related Work

The reverse engineering approach to establish an anatomically realistic neuron population has recently been used to model and analyze the structure (but not the connectivity) of the rat hippocampus [RBA12]. Burysjuk et al. [Bor11] use a similar approach to model a tadpole spinal cord and its connectome, albeit using an axon growth algorithm instead of anatomical reconstructions. No references were found, however, on the modeling of the rat barrel cortex.

Lin et al. [Lin11] present a tool for issuing spatial queries on a database containing reconstructed *Drosophila* neurons registered into an atlas. Although this provides information about neural connectivity based on spatial proximity, it does not permit quantitative conclusions about connectivity strength as this requires realistic estimates of number and type of neurons.

Brain connectivity can be studied at different scales, ranging from the macroscale (connections between brain regions) to the microscale (connections between individual cells). At the mesoscale, connections between medium-sized neuron populations, e.g. cortical columns, are studied [STK05]. Independent of scale the connection pattern can be represented by a graph, which, in the context of connectomics, is often represented by a connectivity matrix. The nodes represent anatomical units, e.g. synapses, neurons, groups of neurons or brain regions, depending on the scale. The links represent connections between the nodes and are either binary, indicating the presence of a connection, or weighted, quantifying the connection strength. The most appropriate way to obtain connectivity information depends on the scale [Pfi12]. At the macroscopic level, fiber tracking of axons in diffusion tensor imaging (DTI) is a technique to identify connections [Hag10]. At smaller scales mainly electron- or light-microscopic techniques with appropriate stains are used [Kle11].

© The Eurographics Association 2012.

Brain networks can be analyzed mathematically (using methods and concepts from the fields of graph/network theory and topology [Kai11]), and /or visually. Creating easily interpretable visualizations of brain networks is non-trivial, as such a network is often a complex graph embedded in 3D. For example, axonal tracts obtained by DTI fiber tracking can be directly rendered in 3D. However, their number and density causes clutter and hampers interpretation, requiring techniques such as abstraction and filtration [JDL12] to create effective visualizations. Being a graph, the connection matrix can be visualized using common graph visualization methods. The most common method is direct visualization by a heatmap (Fig. 1c), where the connection strength between each pair of nodes is color-coded [Bas11]. The main disadvantage is that this visualization provides no spatial context. To aid their interpretation, heatmaps can be complemented by a 3D visualization of the anatomical elements, represented by the nodes. Often these elements are brain regions, e.g. obtained by segmenting MRI data. They are displayed in 3D using surfaces (see e.g. [Ger11, Bas11]) or volume rendering [Guo12], thereby color-coding some network property of the nodes. Alternatively, node-link diagrams based on a force-directed layout algorithm [Hag08] or connectograms [Iri12] are used. These, however, suffer from clutter when network complexity increases. A disadvantage of multiple complementary views is that switching incurs mental effort.

Concluding, at present anatomically realistic 3D models of the rat barrel cortex at cellular resolution do not exist. In addition, general tools for analyzing connectivity information, such as the heatmap or variations of node-link diagrams, have severe drawbacks. Dedicated tools for analyzing multiscale connectivity information between neuron populations within and across cortical columns are lacking.

4. Methods

4.1. Creation of a Barrel Cortex Model

The goal is to create an anatomically realistic model of the excitatory neuron population within the barrel cortex. The 'reverse engineering' approach used in [Obe11a] to model a single column is extended for this purpose. The following anatomical data form the input of the model:

Soma density field, the number of somata per $50 \times 50 \times 50\,\mu m^3$ grid cell. This (preliminary) data is obtained by automatic counting of somata in confocal images, as in [Mey10].

Column metadata of the 24 cortical columns: center, axis (approximately perpendicular to the pia), radius [Egg12] and a label, derived from their position in the barrel field (see Fig. 1b), identified by a row (A–E) and arc (1–4), with additional columns α–δ in front of the first arc.

Cell type metadata of the 10 modeled cell types. Each cell type is named after the cortical layer in which their somata are predominantly located, with an optional subtype indication, e.g. Layer 4 pyramidal (L4py) neurons. Provided is also the number of presynaptic contact sites (boutons, β) per μm axon and the number of postsynaptic contact sites (spines, σ) per μm dendrite. At present, these are given constants (0.33 and 0.5 resp. [Lan11]), and identical for all cell types.

3D morphologies of 10 cell types in 24 columns. Approximately 100 dendritic and $\sim$60 axon morphologies have been reconstructed from brightfield microscopy images [Obe11a, Bru09, Obe11b] and registered into all columns [Egg12], resulting in $\sim$2700 morphologies.

In contrast to the single-column model [Obe11a], care has to be taken to correctly populate the entire region, including the septum. To achieve this, the boundaries between different cell type mixtures have to be defined for the entire region. In addition, the orientation of dendritic morphologies has to be adjusted to point towards the pia.

The mixture of cell types varies with cortical depth. In order to model the correct mixture of cell types at each location, a set of curved, nearly-parallel surfaces bounding different mixture types and spanning the entire barrel field is computed as follows. First, the mixture boundaries within a representative column (e.g. C2) are determined [Obe11a]. To achieve this, the position and cell type is determined for all somata of the dendritic morphologies in the column. Then, the soma positions are projected onto the column axis and binned into $50\,\mu m$ intervals. Finally, the cell type mixture for each interval is computed. When neighboring intervals have different mixtures, a boundary point is defined between them on the column axis. The resulting set of points is transferred to all other column axes, applying a scaling to reflect the differences in column length. A surface between corresponding boundary points on all column axes is created by Delaunay triangulation. Fig. 2a shows the resulting surfaces.

The local dendrite orientation is computed by interpolating the axis direction of the 3 nearest columns at each point. To speed up computation, this local axis direction is precomputed by sampling on a uniform grid A ($50^3\,\mu m^3$ voxels).

Based on this data, the model of the barrel cortex is created as follows. First, a realization of soma positions is computed that satisfies the given soma density field, see Fig. 2b.

Second, each soma is assigned a cell type (Fig. 2c). The mixture region containing a soma is determined by finding the intersection with the boundary surfaces above and below the soma along the direction of the axis of the nearest column. The soma is randomly assigned a cell type satisfying the mixture for this region.

Third, dendrite morphologies are placed at the computed soma positions (Fig. 2d). For each soma, a dendrite morphology, which soma position is close ($< 50\,\mu m$) to the computed soma position, of the assigned cell type and column that is closest to the soma is picked. This morphology is transformed as follows: 1) rotation around the column axis,

© The Eurographics Association 2012.

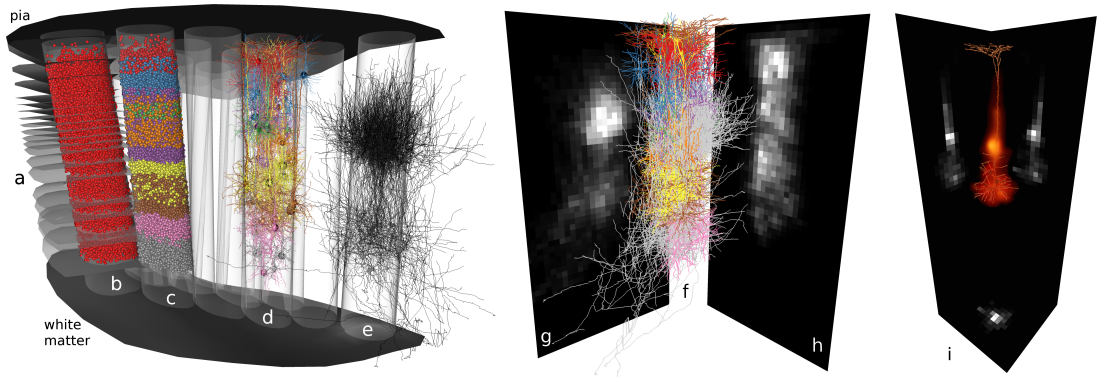

Figure 2: *Left: establishing the barrel field neuron population. For illustrative purposes, each step of the population assembly is shown in a different column and for a small number of morphologies only. a) Mixture region boundary surfaces (clipped). b) Soma distribution inside a column. c) Cell type assignment. d) Dendrite reconstructions, colored by cell type. e) VPM axon reconstructions. Center, right: Illustrative example of the computation of synaptic connectivity for a small neuron population. Maximum intensity projections of the bouton (g) and spine density (h) of the axonal branches of a presynaptic neuron group (f, grey) and dendritic branches of the entire population (f, colored), respectively, sampled on a uniform grid. Based on these numbers, the synapse distribution (i) between a single postsynaptic neuron and the presynaptic group is computed using Eq. (3).*

such that the orientation with respect to the column center is retained; 2) translation of the reconstructed soma position to the new one; 3) scaling along the column axis so the dendrite remains within the column; 4) rotation around the soma, such that the orientation towards the pia surface is retained; the new orientation is looked up in the axis field A.

Finally, reconstructed axons of neuron types for which dendrites are placed are duplicated such that their number equals the number of dendritic reconstructions. VPM axons are also duplicated; their number is determined by counting the somata in their respective thalamic region [Obe11a].

The result of the final step is a population P of axon and dendrite morphologies placed in 3D space. Each morphology has a cell type. Given the definition of the column cylinders, for each dendritic morphology its nearest column is computed and whether its soma is inside or outside this column. This allows us to define groups of morphologies: a group $G^{(ct,col)}$ consists of all neurons of cell type ct having their soma inside column col. In addition, we define the groups $G^{(VPM,col)}$ consisting of VPM cells, whose somata are located in the thalamus instead of the columns, but have axons projecting mainly into their respective columns col.

4.2. Computation of Synaptic Connectivity

Synapse numbers are estimated based on structural overlap between axons and dendrites, commonly referred to as Peters' rule [Pet79]. The volume V containing all neurons is therefore partitioned into a uniform grid of volumetric elements (of grid cell size $50^3\,\mu m^3$ in our case, related to the registration error of the morphologies into barrel field reference system [Egg12]). Specifically, the number of synapses is determined by dividing the local number of presynaptic contact sites (boutons) on the axons among the local number of postsynaptic contact sites (spines) on the dendrites. Given the bouton and spine densities β, σ, the number of boutons $B(c,\mathbf{x})$ of neuron c within grid cell $\mathbf{x}$ is $B(c,\mathbf{x}) = \beta \cdot L_{axon}(c,\mathbf{x})$, where $L_{axon}(c,\mathbf{x})$ is the axon length of c in $\mathbf{x}$. The number of spines $SP(c,\mathbf{x})$ is, analogously, $SP(c,\mathbf{x}) = \sigma \cdot L_{dendrite}(c,\mathbf{x})$. The number of boutons of an entire presynaptic group is obtained by summing over all neurons in the group:

$$B(G_{pre},\mathbf{x}) = \sum_{i \in G_{pre}} B(i,\mathbf{x}), \tag{1}$$

and for the number of spines of the entire population:

$$SP(P,\mathbf{x}) = \sum_{j \in P} SP(j,\mathbf{x}). \tag{2}$$

The number of synaptic contacts $S(G_{pre},c,\mathbf{x})$ of a presynaptic neuron group G_{pre} with a postsynaptic cell c within grid cell $\mathbf{x}$ is computed as follows:

$$S(G_{pre},c,\mathbf{x}) = SP(c,\mathbf{x}) \cdot \frac{B(G_{pre},\mathbf{x})}{SP(P,\mathbf{x})} \tag{3}$$

From these single-cell synapse distributions, we can compute different statistical quantities of interest, e.g. the total number of synapses $S(G_{pre},c)$ of c with a presynaptic group:

$$S(G_{pre},c) = \sum_{\mathbf{x} \in V} S(G_{pre},c,\mathbf{x}), \tag{4}$$

or the total number of synapses of a postsynaptic group with a presynaptic group:

$$S(G_{pre},G_{post}) = \sum_{c \in G_{post}} S(G_{pre},c). \tag{5}$$

© The Eurographics Association 2012.

Dividing by the number of postsynaptic cells $|G_{post}|$ results in the average number of synapses per postsynaptic cell:

$$\hat{S}(G_{pre}, G_{post}) = \frac{1}{|G_{post}|} \sum_{c \in G_{post}} S(G_{pre}, c). \qquad (6)$$

Computing $S(G_{pre}, G_{post})$ for all combinations of pre- and postsynaptic groups results in a connectivity matrix M, representing the total number of synapses between each pair of groups. This can be done analogously for the matrix $\hat{M}$ consisting of $\hat{S}(G_{pre}, G_{post})$ entries.

4.3. Framework for Visual Analysis of Synaptic Connectivity at Multiple Scales

The framework consists of multiple coordinated views and follows the Model-View-Controller paradigm. The model consists of:

- neuron population P,
- network metadata: column geometry and cell type properties (e.g. bouton/spine density),
- synapse evaluator proxy providing values of connectivity matrices M, $\hat{M}$ and synapse densities for the 3D view,
- selection of pre- and postsynaptic groups $\{G_{pre}\}$, resp. $\{G_{post}\}$,
- and a selected postsynaptic neuron $c \in \{G_{post}\}$.

To ensure interactive response times, the connectivity matrix values are precomputed. The 3D synapse distributions are computed on-the-fly using cached values of frequently used fields (population spine density grid $SP(P, \mathbf{x})$ and bouton densities for all groups $B(G_{pre}, \mathbf{x})$).

The framework presents the user the following views:

- Cortical Column Connectivity View (CCCV),
- 3D view showing the synapse density as well as synapse distributions on the dendrites of individual neurons,
- heatmap view of a connectivity matrix (requested by user, because it is a familiar standard visualization).

Whereas the CCCV and the heatmap visualize connectivity at the scale of cell populations, the 3D view shows synaptic innervation at the subcellular scale. Both the heatmap and the CCCV can display either the values of M or $\hat{M}$. The user can explore the connectivity information by interactively defining selections $\{G_{pre}\}$ and $\{G_{post}\}$ for which the synapse information is to be shown in the CCCV. This can be done either in the CCCV or in the heatmap; the selection is automatically propagated to the other view (in the heatmap, the selection is simply highlighted, as it always shows the entire matrix). In addition, a single neuron of any of the selected postsynaptic groups can be selected, for which the synapse distribution is displayed in detail in the 3D view. Single neurons can be selected by picking from a list, sorted by neuron group. By iteratively modifying the selection in a targeted manner the user can drill down in the data, while increasing insight. The framework is implemented in ZIBAmira (http://amira.zib.de).

4.4. Cortical Column Connectivity View

To overcome the main disadvantage of the heatmap (no spatial reference), we devised a visualization that presents the essential connectivity information within and between cortical columns in a semi-spatial context. In the CCCV, the columns are displayed in 2D as contours (Fig. 3a). Their position approximates their relative position within the cortical sheet (Fig. 1b), thus creating a spatial reference. A more exact mapping of the cortical sheet to the 2D plane would be conceivable, but for our application this approximation sufficed. In each contour the pre- and postsynaptic connectivity values are displayed as bars. The vertical ordering of the cell types follows the cortical layering and is therefore a rough approximation of the spatial column axes (Fig. 3c).

The user explores the connectivity information by interactively specifying selections $\{G_{pre}\}$ and $\{G_{post}\}$ (Fig. 3b,c). When a selection has been defined, the bars on the left side of each column show for each selected presynaptic neuron group the sum of synapses this group projects to. Conversely, the bars on the right side display the sum of synapses each postsynaptic group receives from the selected presynaptic groups. The sum of all values on the presynaptic side thus always equals the sum of values on the postsynapic side.

4.5. 3D View of Subcellular Synapse Distributions

The purpose of the 3D view is two-fold: first, it visualizes subcellular differences in synaptic density by coloring the morphology of a selected postsynaptic neuron c by the local synapse density $S(\{G_{pre}\}, c, \mathbf{x})$ (see Fig. 5a). Second, it shows the distribution of synapses on the dendritic branches of c, colored by presynaptic cell type, in order to identify subcellular regions of preferred synaptic innervation for different presynaptic cell types (Fig. 5b).

The synapse positions are determined by randomly placing $S(G_{pre}, c, \mathbf{x})$ synapses on the dendrites of c within the $50^3\,\mu m^3$ grid cell $\mathbf{x}$, for each $G_{pre} \in \{G_{pre}\}$. When more detailed information concerning the true distribution along the dendrites becomes available, this can be incorporated.

5. Application Example

To show how the framework is used to obtain insight into the synaptic connectivity in the barrel cortex model, we apply it to answer the questions posed in Section 2.

In order to quantify thalamic input into the barrel cortex (Q1, Q2), we select all presynaptic VPM groups by clicking on the PRE-VPM box (Fig. 3b). The total presynaptic number of synapses of these groups is indicated by the black bars in Fig. 3a. We observe that the VPM cells corresponding to the central columns and the E-row provide most input, and that the cells in these columns receive most input. Further we observe, that the relative amount of synapses per postsynaptic group is similar for each column: Layer 4 star pyramids

© The Eurographics Association 2012.

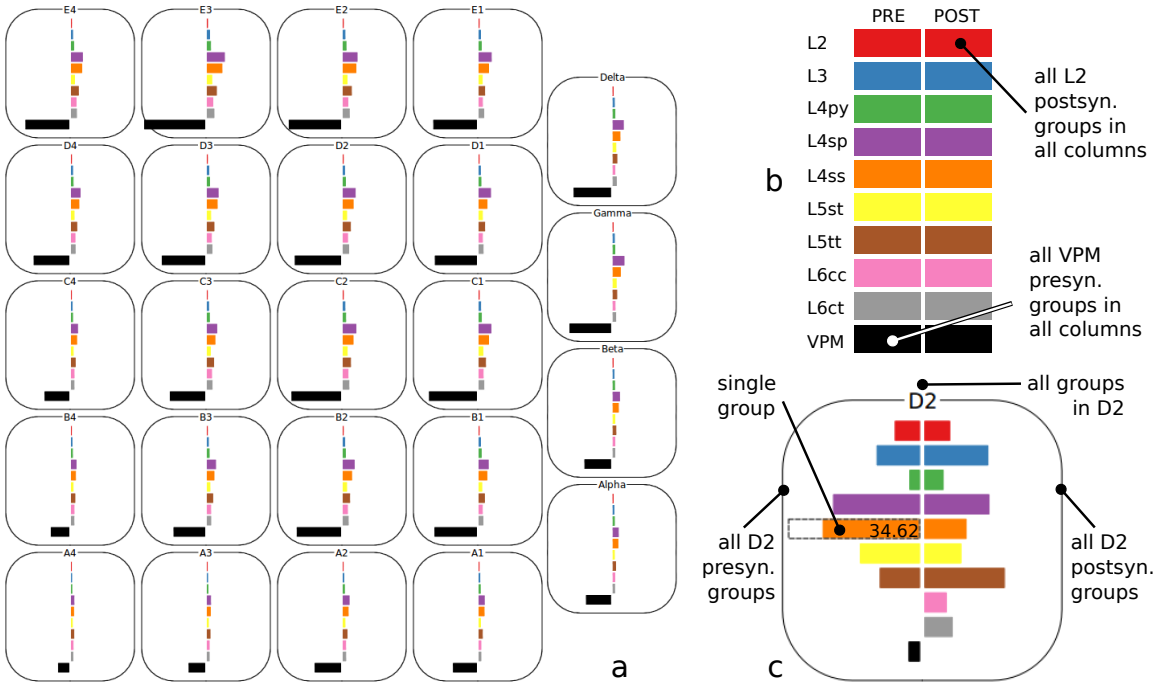

Figure 3: *(a) The CCCV lays out all columns according to their position in the cortical sheet. The bars show the number of synapses selected that presynaptic groups (left, here: all VPM groups) share with selected postsynaptic groups (right, here: all other cell types). (b) cell type legend that is displayed as part of the CCCV, and which can be used to make selections. (c) One example column in the CCCV. The rendered elements can be used for defining selections. Here the presynaptic L4ss group of column D2 has been selected (as indicated by the dashed line). Multi-selection is achieved by holding a modifier key. Values can be displayed as text (only one value shown for illustration).*

(L4sp) and spiny stellates (L4ss) receive most input, whereas L2 and L3 cells hardly receive any (as reported in [Obe11a]).

To reveal how one of the central columns (D2) is innervated by its corresponding VPM axons (Q1), we select the presynaptic D2-VPM group and all postsynaptic D2 groups (Fig. 4a). Again we observe that L4sp and L4ss receive the largest number of synapses from VPM (indicated by the red arrows). To determine whether this is due to the large number of neurons in these two groups, we display the average number of synapses per postsynaptic neuron (Fig. 4b) and observe that this is the case, and that among all cell types actually Layer 4 pyramids (L4py) receive most synapses per cell from VPM.

To find out what other cell types a L4py neuron gets input from (Q1), we select all presynaptic groups and the postsynaptic L4py group in D2. Most input is due to L4ss and L4sp (Fig. 4c, red arrows). As pyramidal cells have distinct dendritic compartments with short, highly arborized basal dendrites around the soma and a long apical dendrite extending towards the pia, we ask whether there is cell-type specific clustering of synapse positions on the dendrites (Q3). We therefore switch to the 3D view, select a L4py cell and observe that synapses are densest close to the soma (Fig. 5a). The main input types are L4ss and L4sp. Restraining the selection to these types and showing the synapse positions (5b) reveals that these cell types mainly innervate the basal dendrites. This raises the question what cell types connect to the apical dendrite. We broaden the selection to all presynaptic cell types and zoom in on the apical tuft (5c). The L2, L3 and L5 slender-tufted (L5st) cells seem to dominate the synaptic input to the tuft. Indeed, if we look at the L2-L4py synapses only (5d,e), we observe that L2 predominantly innervates the apical dendrite.

What cells does L2 receive input from, when not from VPM? Selecting the postsynaptic L2 group in D2 immediately provides the answer (not shown due to space limitations). To differentiate between intra-column input and input from surrounding columns (Q4), we first select all presynaptic D2 cell types and observe that L2 in D2 is innervated by ∼3.8 million synapses (Fig. 4d). Selecting all presynaptic cell types in the columns surrounding D2 reveals that L2 in D2 receives more input from neighboring columns (∼4.3 million synapses), mainly from L5st (4e).

© The Eurographics Association 2012.

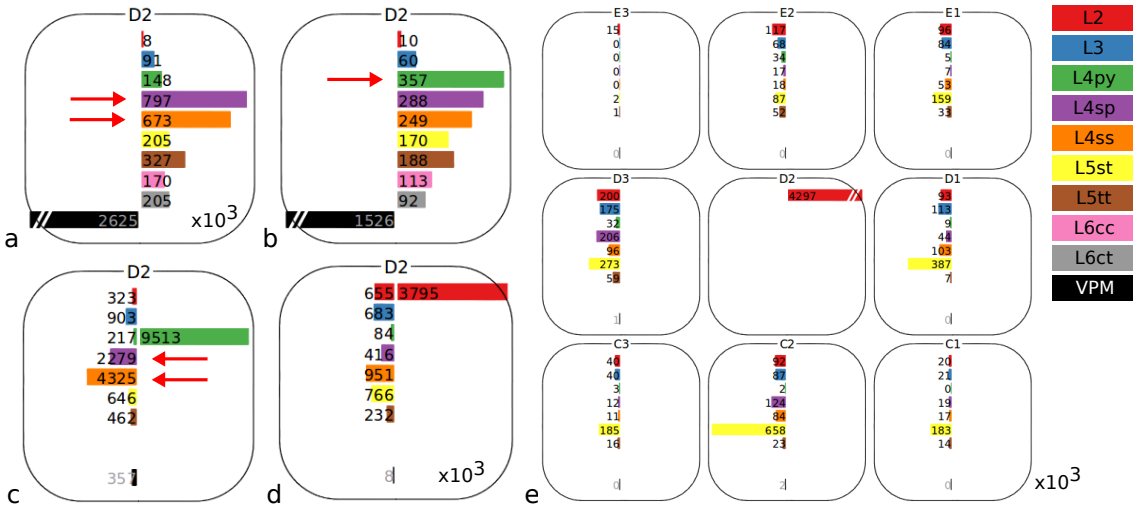

Figure 4: *(a) Total number of VPM synapses with D2 cell types.(b) Average number of VPM synapses. (c) Average number of synapses that an L4py neuron receives from other cell types in D2. (d) Intra-column L2 innervation (total synapses). (e) L2 input from surrounding columns.*

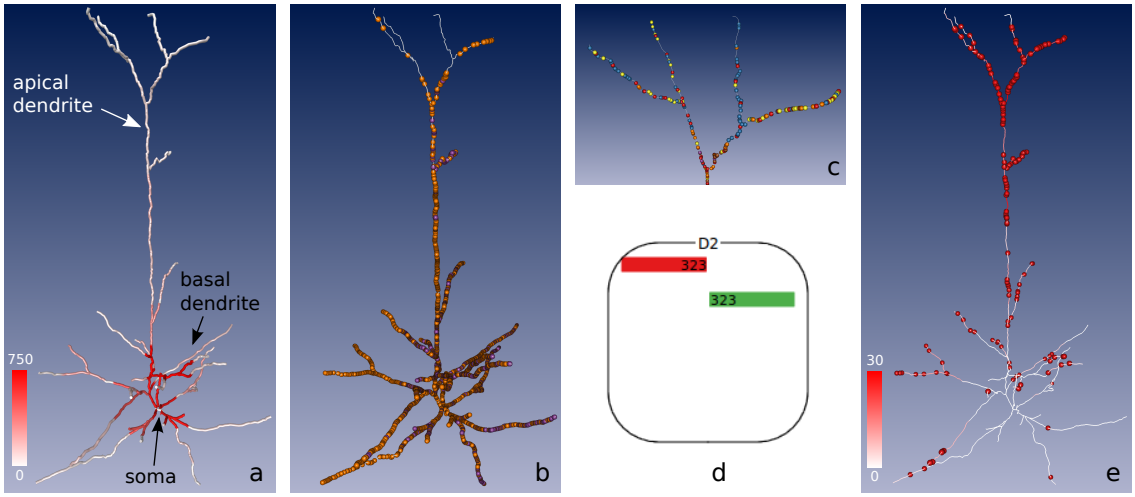

Figure 5: *(a) Synapse density color-coded on L4py dendrites. (b) Synapse positions of presynaptic L4ss and L4sp cells. (c) Synapses on apical tuft. (d) Number of synapses for the L2-L4py connection in the CCCV. (e) L2 synapse positions.*

6. Discussion

The barrel cortex model described here enables the study of its (sub)cellular architecture region and synaptic connections. The most important assumptions for model validity are that (i) the reconstructed morphologies are a representative sample of the true population and that (ii) the computation of the synaptic connectivity based on Peters' rule is a good estimate. See [Obe11a] for a more detailed discussion.

The information displayed by the CCCV is to a large extent the same as a heatmap representation. The main differences are the aggregation of connectivity matrix values when more than one pre- or postsynaptic group is selected, and the semi-spatial context, aiding localization and the investigation of the interaction between columns. Whether it can replace the heatmap, which is more generally applicable and currently the familiar standard representation, remains to be seen. However, as they share the same data structure (the connectivity matrix) they can easily be used side-by-side in an integrated framework. The CCCV is not limited to the barrel cortex, but can be used for all regions located on a curved 2D surface, such as the cortical sheet. The size of the brain region that can be studied using the CCCV is, however, limited by the number of columns that fit on the screen.

© The Eurographics Association 2012.

While the framework presented here allows to study connectivity from the level of synapses and individual neurons up to cortical areas containing several dozens of columns, such as S1, larger models spanning more scales and eventually representing entire brains will undoubtedly be developed. Their investigation requires visualization tools that extend the multiscale approach to the entire hierarchy.

The modeling approach and the visualization framework are considered very useful by domain experts from the Max Planck Florida Institute: "This set of tools allows scientists to investigate structural organization principles at the scale of an entire cortical area with sub-cellular resolution. In particular cell type- and location-specific connectivity patterns are accessible for the first time, and may be extended and/or compared to more direct connectivity measurements from electron microscopy. The 2D layout of columns and cell types is a great advantage of the CCCV over the heatmap representation as it aids in localization and understanding of column interactions. The various selection options make query specification simple, resulting in short question/response iterations. It is therefore fun to work with."

7. Conclusion

We extended an existing reverse engineering approach [Obe11a] to create a neural network model of the rat barrel cortex and its synaptic connections. The presented visualization framework offers a highly interactive tool to explore the complex connection patterns contained in such models at multiple scales. The CCCV is a new interactive tool to investigate connections between groups of cells in different cortical columns. A 3D view shows synapse positions on individual neurons. We showed that the framework aids neuroscientists in answering important biological questions. We believe that such a multiscale visualization approach is a promising direction to obtain insight in connectomics data of ever-increasing size and complexity.

Acknowledgements

We would like to thank Bert Sakmann (Max Planck Florida Institute) for advice and proof-reading, as well as Marianne Krabi (Zuse Institute Berlin) for implementation assistance.

References

[Bas11] BASSETT D.S., ET AL.: Conserved and variable architecture of human white matter connectivity. *NeuroImage 54*, 2 (2011), 1262–1279. 3

[Bor11] BORISYUK R., ET AL.: Modeling the connectome of a simple spinal cord. *Front Neuroinform 5* (2011), 20. 2

[Bru09] BRUNO R.M., ET AL.: Sensory experience alters specific branches of individual corticocortical axons during development. *J Neurosci 29*, 10 (2009), 3172–3181. 3

[CS07] CELIKEL T., SAKMANN B.: Sensory integration across space and in time for decision making in the somatosensory system of rodents. *PNAS 104*, 4 (2007), 1395–1400. 1

[Egg12] EGGER R., ET AL.: 3D Reconstruction and Standardization of the Rat Vibrissal Cortex for Precise Registration of Single Neuron Morphology. *Submitted* (2012). 3, 4

[Ger11] GERHARD S., ET AL.: The Connectome Viewer Toolkit: An Open Source Framework to Manage, Analyze, and Visualize Connectomes. *Front Neuroinform 5*, 3 (2011), 1–15. 3

[Guo12] GUO Y., ET AL.: Pattern Visualization of Human Connectome Data. In *EuroVis - Short Papers* (Vienna, Austria, 2012), Weinkauf T., Meyer M., (Eds.), pp. 78–83. 3

[Hag08] HAGMANN P., ET AL.: Mapping the structural core of human cerebral cortex. *PLoS Biol 6*, 7 (2008), e159. 3

[Hag10] HAGMANN P., ET AL.: MR connectomics: Principles and challenges. *J Neurosci Meth 194* (2010), 34–45. 2

[Hel07] HELMSTAEDTER M., ET AL.: Reconstruction of an average cortical column in silico. *Brain Res Rev 55*, 2 (2007), 193–203. 1, 2

[Iri12] IRIMIA A., ET AL.: Patient-tailored connectomics visualization for the assessment of white matter atrophy in traumatic brain injury. *Front Neurol 3*, 10 (2012), 1–21. 3

[JDL12] JIANU R., DEMIRALP C., LAIDLAW D. H.: Exploring Brain Connectivity with Two-Dimensional Neural Maps. *IEEE T Vis Comput Gr 18*, 6 (2012), 978–987. 3

[Kai11] KAISER M.: A tutorial in connectome analysis: Topological and spatial features of brain networks. *NeuroImage 57*, 3 (2011), 892–907. 3

[Kle11] KLEINFELD D., ET AL.: Large-scale automated histology in the pursuit of connectomes. *J Neurosci 31*, 45 (2011), 16125–16138. 2

[Lan11] LANG S., ET AL.: Simulation of Signal Flow in Three-Dimensional Reconstructions of an Anatomically Realistic Neuronal Network in Rat Vibrissal Cortex. *Neural Networks 24*, 9 (2011), 998–1011. 1, 3

[Lin11] LIN C-Y., ET AL.: The Neuron Navigator: Exploring the Information Pathway through the Neural Maze. In *IEEE Pacific Visualization Symposium* (2011), IEEE, pp. 35–42. 2

[Mey10] MEYER H.S., ET AL.: Number and Laminar Distribution of Neurons in a Thalamocortical Projection Column of Rat Vibrissal Cortex. *Cereb Cortex 20*, 10 (2010), 2277–2286. 3

[Obe11a] OBERLAENDER M., ET AL.: Cell Type-Specific Three-Dimensional Structure of Thalamocortical Circuits in a Column of Rat Vibrissal Cortex. *Cereb Cortex* (2011). doi:10.1093/cercor/bhr317. 1, 3, 4, 6, 7, 8

[Obe11b] OBERLAENDER M., ET AL.: Three-dimensional axon morphologies of individual layer 5 neurons indicate cell type-specific intracortical pathways for whisker motion and touch. *P Natl Acad Sci USA 108*, 10 (2011), 4188–4193. 3

[Pet79] PETERS A.: Thalamic input to the cerebral cortex. *Trends Neurosci 2* (1979), 1183–1185. 4

[Pfi12] PFISTER H., ET AL.: *Visualization in Connectomics*. Tech. rep., 2012. URL: http://arxiv.org/abs/1206.1428. 2

[RBA12] ROPIREDDY D., BACHUS S. E., ASCOLI G. A.: Nonhomogeneous stereological properties of the rat hippocampus from high-resolution 3D serial reconstruction of thin histological sections. *J Neurosci 205* (2012), 91–111. 2

[STK05] SPORNS O., TONONI G., KÖTTER R.: The Human Connectome: A Structural Description of the Human Brain. *PLoS Comput Biol 1*, 4 (2005), e42. 1, 2

[Var11] VARGA Z., ET AL.: Dendritic coding of multiple sensory inputs in single cortical neurons in vivo. *PNAS 108*, 37 (2011), 15420–15425. 2

© The Eurographics Association 2012.